Hindawi Publishing Corporation
Journal of Nanomaterials
Volume 2015, Article ID 917935, 6 pages
http://dx.doi.org/10.1155/2015/917935

Research Article

The Reliability Improvement of Cu Interconnection by the Control of Crystallized α-Ta/TaN$_x$ Diffusion Barrier

Wei-Lin Wang,[1] Chia-Ti Wang,[2] Wei-Chun Chen,[3] Kuo-Tzu Peng,[1] Ming-Hsin Yeh,[1] Hsien-Chang Kuo,[1] Hung-Ju Chien,[1] Jen-Chi Chuang,[2] and Tzung-Hua Ying[1]

[1]*Process Technology Development Division, Powerchip Technology Corporation, Hsinchu Science Park, Hsinchu 30078, Taiwan*
[2]*Logic Technology Development Division, Powerchip Technology Corporation, Hsinchu Science Park, Hsinchu 30078, Taiwan*
[3]*Instrument Technology Research Center, National Applied Research Laboratories, Hsinchu, Taiwan*

Correspondence should be addressed to Wei-Lin Wang; wwl@powerchip.com and Wei-Chun Chen; weichun@narlabs.org.tw

Received 27 October 2014; Revised 14 February 2015; Accepted 15 February 2015

Academic Editor: Zhenbo Wang

Ta/TaN bilayers have been deposited by a commercial self-ionized plasma (SIP) system. The microstructures of Ta/TaN bilayers have been systematically characterized by X-ray diffraction patterns and cross-sectional transmission electron microscopy. TaN films deposited by SIP system are amorphous. The crystalline behavior of Ta film can be controlled by the N concentration of underlying TaN film. On amorphous TaN film with low N concentration, overdeposited Ta film is the mixture of α- and β-phases with amorphous-like structure. Increasing the N concentration of amorphous TaN underlayer successfully leads upper Ta film to form pure α-phase. For the practical application, the electrical property and reliability of Cu interconnection structure have been investigated by utilizing various types of Ta/TaN diffusion barrier. The diffusion barrier fabricated by the combination of crystallized α-Ta and TaN with high N concentration efficiently reduces the KRc and improves the EM resistance of Cu interconnection structure.

1. Introduction

For the Cu interconnection process of current integrated circuit (IC) devices, Ta/TaN bilayer is commonly used as diffusion barrier between Cu metal line and dielectric oxide layer. The purpose of Ta film is the adhesion with Cu line. For the adhesion with dielectric oxide layer, TaN presents superior ability [1, 2]. In multilevel Cu interconnection process, Ta/TaN diffusion barriers are also deposited between Cu via bottoms and underlying Cu lines. Thus, the resistance of Ta/TaN diffusion barrier inevitably impacts the contact resistance (Rc) of Cu interconnection structure. As IC device scaled down drastically, the Rc of Cu interconnection is expected to increase. Hence, the fabrication of Ta/TaN diffusion barrier with low resistance is crucial for upholding device speed. In addition to Rc issue, electromigration (EM) resistance is affected by the resistance of Ta/TaN diffusion barrier. During the operation of IC device, EM occurs due to the interaction of various atomic fluxes which can be induced by electron-wind force, stress gradient, and temperature. The electron-wind force is particularly enhanced when electrons flow from high resistance region to low resistance region. Therefore, the atomic flux divergence resulting from electron-wind force is easily magnified by the high resistance diffusion barrier between Cu via bottom and underlying Cu line [3, 4]. Clearly, the reliability issue strongly depends on the electrical property of Ta/TaN diffusion barrier. Lowering the resistance of Ta/TaN diffusion barrier is desirable for the improvement of Cu interconnection reliability.

For Ta metal, there are two types of crystal phases, including α-phase Ta (α-Ta) and β-phase Ta (β-Ta). Generally, bulk Ta metal is α-Ta which is body-centered cubic structure with resistivity about 15~60 $\mu\Omega$cm. The metastable phase, β-Ta, is tetragonal structure with resistivity in the range of 170~210 $\mu\Omega$cm [5, 6]. In the practical application for IC devices, β-Ta is undesirable because of its high resistivity. However, the formation of β-Ta is easily found in Ta thin film deposited by sputtering system [7, 8]. In contradiction, sputtering system is widely utilized in the deposition process of Ta/TaN diffusion barrier. In order to reduce Rc and avoid EM-induced voids

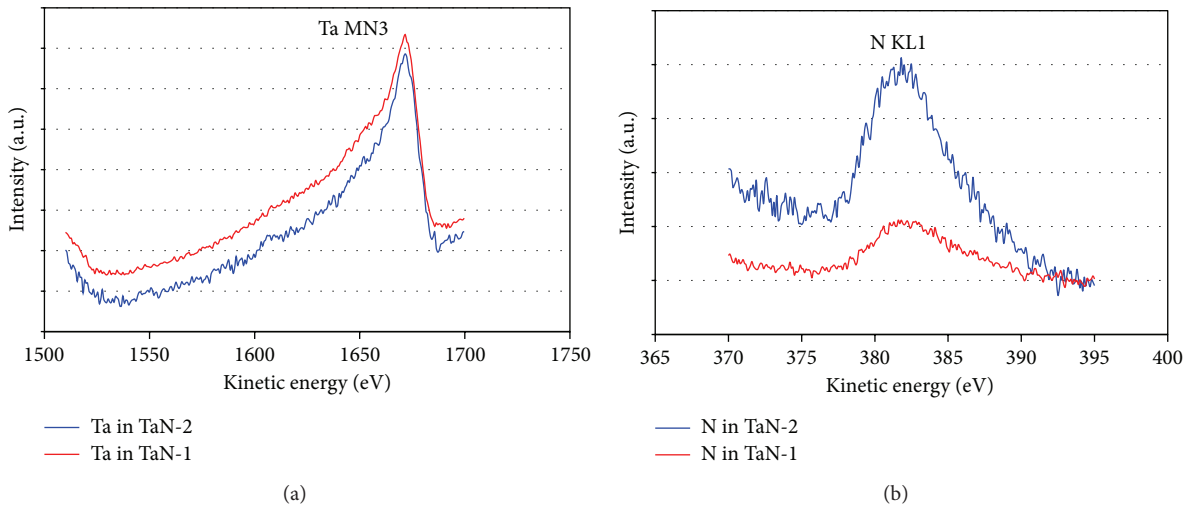

Figure 1: The AES spectra of (a) Ta MN3 and (b) N KL1 taken from TaN-1 and TaN-2 films deposited on SiO_2.

in Cu interconnection, the fabrication of α-Ta film therefore becomes the goal of many researches. The preparation of α-Ta film was demonstrated by various methods, such as the adjustment of N_2/Ar ratio, phase transformation by thermal treatment, TaN surface treatment, and the increment of N concentration in TaN film [9–12]. Although α-Ta film was successfully achieved by using the abovementioned methods in sputtering system, the grain boundaries of the α-Ta film were verified to be the potential paths for Cu diffusing into dielectric oxide layer [13]. By considering the purpose of diffusion prevention, amorphous TaN underlayer is a promising candidate. Accordingly, an ideal diffusion barrier structure is supposed to consist of crystallized α-Ta and amorphous TaN films.

In this study, Ta/TaN bilayers were deposited by sputtering system. Amorphous TaN films with various N concentration levels were prepared to control the crystal phases of overdeposited Ta films. For the practical application, the electrical performances of Cu interconnection structures were investigated by using three types of Ta/TaN diffusion barriers.

2. Experimental Procedure

TaN and Ta/TaN films were deposited on 12-inch SiO_2/Si wafers. A commercial self-ionized plasma (SIP) system was chosen for thin film deposition. For TaN and Ta/TaN films, the deposition processes were operated under room temperature. In order to realize and control the crystal behavior of Ta film, two TaN films varying in N concentration were prepared and defined as TaN-1 and TaN-2. For the processes of Ta/TaN-1 and Ta/TaN-2 bilayers, Ta films were subsequently deposited on TaN underlayer with N_2 flow rate immediately switched to 0 sccm. On TaN-1 and TaN-2 films, all Ta films were deposited with the same condition. The thickness of thin film was estimated by deposition rate. For wafer-to-wafer, the thickness deviation was controlled to be less than 1 nm. A VG scientific Microlab 350 Auger electron spectroscopy (AES) was employed to determine the chemical composition proportions of TaN-1 and TaN-2 films. The crystal properties of thin films were investigated by grazing incident X-ray diffraction (GIXRD) measurement in a Bede D1 X-ray diffractometer equipped with Cu$K\alpha$ X-ray tube. The incident angle of GIXRD was kept at 3° for all samples. The microstructures of Ta/TaN bilayer films were observed by a Philip Tecnai G2 transmission electron microscopy (TEM) with field emission gun operated at 200 kV. The preparation of cross-sectional TEM (XTEM) specimen was accomplished in a FEI Nova 200 focused ion beam instrument with dual beam system.

For the realistic performances of diffusion barriers, three types of Ta/TaN diffusion barriers were incorporated into Cu interconnection structures. There were Ta/TaN-1, Ta/TaN-2, and Ta/TaN-3 diffusion barriers. Ta/TaN-1 and Ta/TaN-2 were fabricated with nearly the same thickness. The deposition condition of TaN-3 was identical with TaN-1. The thickness of Ta film on TaN-3 was set as only a half of that on TaN-1 and TaN-2. Kelvin contact resistance (KRc) measurements were carried out for evaluating the performances of three Ta/TaN diffusion barriers in Cu interconnection structures. The effects of three Ta/TaN diffusion barriers on the reliability issues of Cu interconnection structures were confirmed by EM test. The EM resistance was tested under high temperature. The failure criterion of EM test was resistance shift more than 10%.

3. Results and Discussion

For defining the composition ratio of various TaN films on SiO_2, the AES spectra of Ta MN3 and N KL1 signals are shown in Figures 1(a) and 1(b). In Figure 1(a), the Ta spectrum of TaN-1 film exhibits stronger intensity than that of TaN-2 film. Oppositely, TaN-2 film gives higher N signal intensity than TaN-1 film as seen in Figure 1(b). Based on the results of AES chemical analyses, TaN-2 film contains higher N concentration than TaN-1 film. By calculating the integral

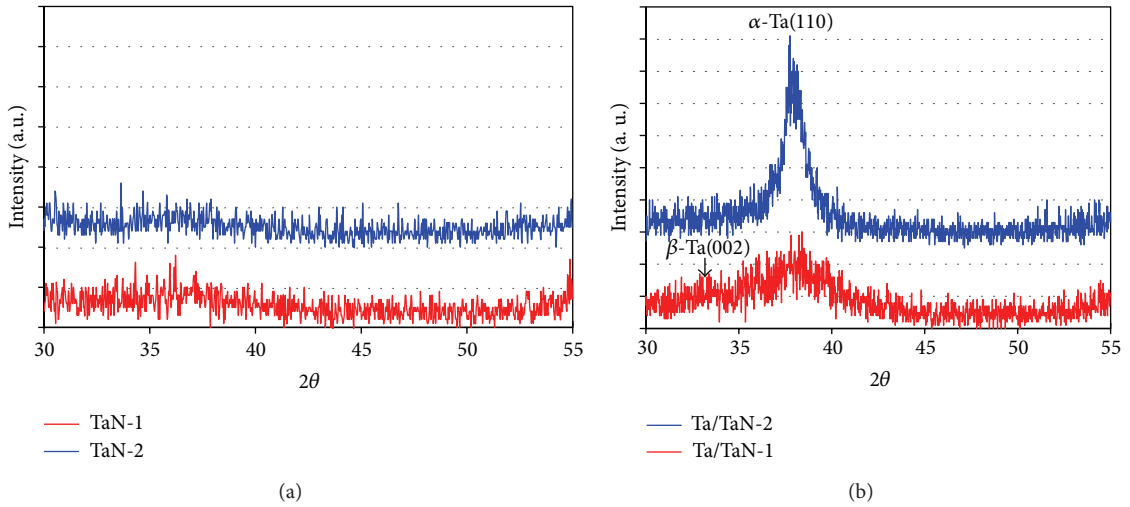

FIGURE 2: The XRD patterns of (a) TaN-1 and TaN-2 films and (b) Ta/TaN-1 and Ta/TaN-2 bilayers deposited on SiO_2.

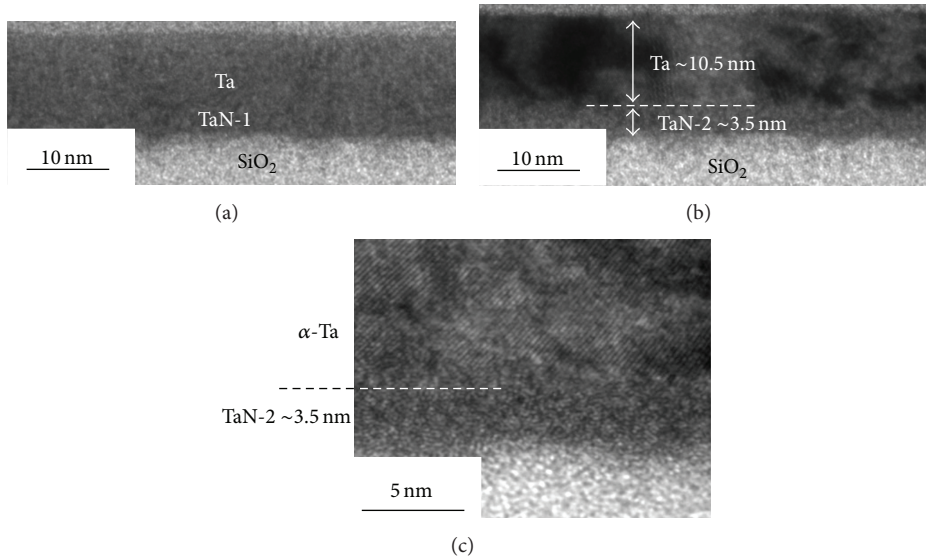

FIGURE 3: The XTEM images of (a) Ta/TaN-1 and (b) Ta/TaN-2 bilayers deposited on SiO_2. (c) The HR-XTEM image of Ta/TaN-2 interface.

area ratios of Ta MN3 and N KL1 peaks, the N concentration is only 10% in TaN-1 film. The N concentration of TaN-2 film is about 30%.

The crystalline properties of TaN films and Ta/TaN bilayers on blanket SiO_2/Si wafers are revealed by the XRD patterns. In Figure 2(a), the XRD patterns of TaN-1 and TaN-2 films appear without any specific diffraction peaks. Evidently, both TaN-1 and TaN-2 films are amorphous. The influence of N concentration in TaN film on the crystal behavior of overdeposited Ta film is realized by the XRD patterns in Figure 2(b). For Ta film deposited on TaN-1 underlayer, the XRD diffraction peaks are weak and broad. The XRD peaks located near 33.7° and 38.4° are indexed as β-Ta(002) and α-Ta(110). According to the profile of the XRD pattern taken from Ta/TaN-1, the Ta film is the mixture of α-Ta and β-Ta in which the structure is destitute of sufficient crystallization and nearly amorphous. In contrast, the Ta film deposited on TaN-2 underlayer shows a strong and sharp α-Ta(110) peak. Apparently, increasing the N concentration of TaN film is beneficial for upper Ta film to form pure α-phase. Previous literature reported by Wang et al. indicated that Ta film with pure α-phase could form after increasing N concentration of underlying TaN film. It concluded that TaN surface with high N concentration could deliver sufficient driving force for subsequent Ta atoms to arrange in the order of α-phase structure [11]. Thus, the crystallization behavior of Ta film is controllable through the adjustment of TaN_x underlayer.

To further clarify the microstructures of Ta/TaN-1 and Ta/TaN-2 bilayers deposited on blanket SiO_2/Si wafers, Figures 3(a)~3(b) give the corresponding bright field XTEM (BF-XTEM) images. Figure 3(a) is the BF-XTEM image of Ta/TaN-1. The homogenous diffraction contrast of amorphous-like and amorphous structures gives the difficulty in the confirmation of Ta/TaN-1 interface.

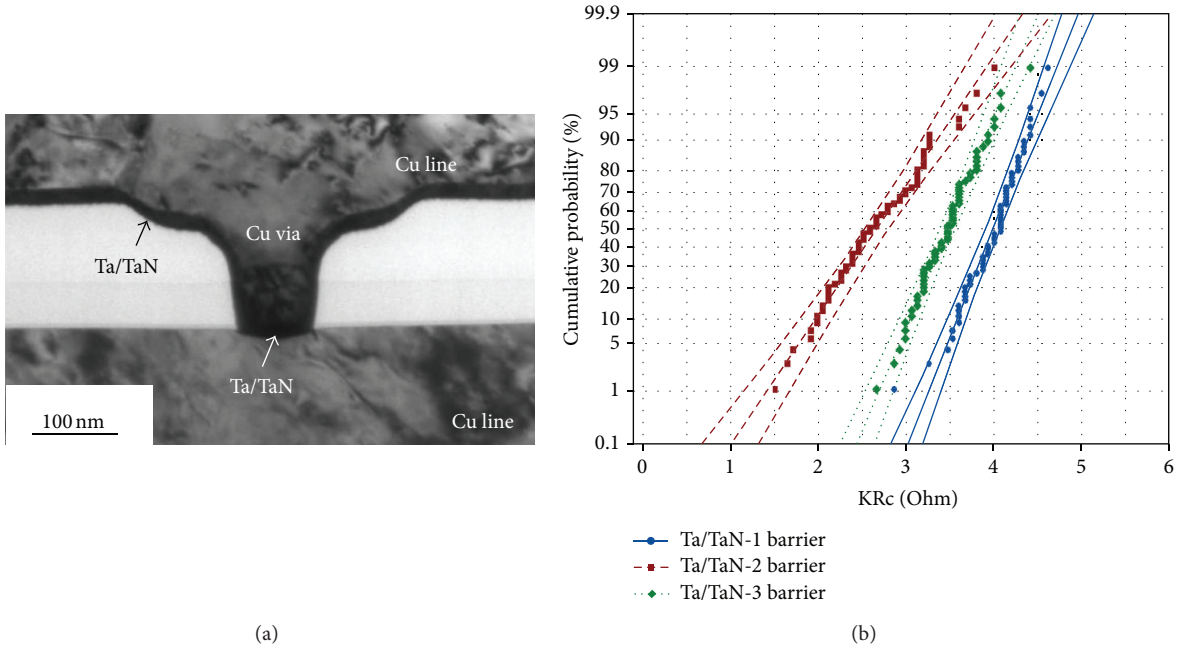

(a) (b)

FIGURE 4: (a) The typical XTEM image of a test Cu interconnection structure. (b) The cumulative probability plot of the KRc measured from the test structures with Ta/TaN-1, Ta/TaN-2, and Ta/TaN-3 diffusion barriers.

Although the N concentration of underlying TaN-1 is 10%, the elementary contrast is almost bare. Unlike Ta/TaN-1 bilayer, Ta film with complete crystallization on TaN-2 shows clear diffraction contrast which is produced by various orientations of α-Ta grains as observed in Figure 3(b). The diffraction contrast unambiguously defines the bilayer structure and interface of Ta/TaN-2. In the bilayer structure of Ta/TaN-2, Ta and TaN are about 10.5 nm and 3.5 nm. Figure 3(c) shows the high resolution XTEM (HR-XTEM) image taken from the interfacial region of Ta/TaN-2 bilayer. In the HR-XTEM image of Figure 3(c), the HR lattice fringes of α-Ta crystal and the amorphous fringes of underlying TaN are clearly distinguishable. The interface positions of α-Ta and amorphous TaN are determined by the dashed line. The results of XTEM observations are consistent with the conclusions of XRD analyses.

In order to realize the performance of Ta/TaN bilayer in the practical application, the test structure of Cu interconnection is exhibited in Figure 4(a). Three types of Ta/TaN diffusion barriers are hereby presented to investigate the influences on the electrical properties of Cu interconnection structures. On KRc measurements, the fabrication of Ta/TaN-1 and Ta/TaN-2 diffusion barriers is used for understanding the effect of Ta crystal phase. The effect of barrier thickness is studied by Ta/TaN-3 diffusion barrier. Figure 4(b) is the cumulative probability plot of the KRc results measured from the Cu interconnection structures with various Ta/TaN diffusion barriers. As seen in the plot, the KRc of the test structure with Ta/TaN-3 diffusion barrier is lower than that with Ta/TaN-1 diffusion barrier. The Cu interconnection structure inserted with Ta/TaN-2 diffusion barrier has the lowest KRc among all test structures. For the test structures with Ta/TaN-1, Ta/TaN-2, and Ta/TaN-3 diffusion barriers, the mean KRc values are 4.04 Ω, 2.78 Ω, and 3.37 Ω, respectively. Based on the KRc measurements, thinning the thickness of Ta/TaN diffusion barrier is helpful to decrease the KRc of Cu interconnection. However, the utilization of α-Ta/TaN diffusion barrier significantly reduces the overall KRc more efficiently. For Ta metal, the resistivity of α-phase is much lower than that of β-phase or the mixture of α- and β-phases. Thus, α-Ta/TaN barrier can provide lower KRc than decreasing the thickness of Ta/TaN barrier with mixed phases.

The reliability issue of Cu interconnection is also discussed with three types of Ta/TaN diffusion barriers. For Cu interconnection, one of the most important reliability issues is EM resistance. In EM test, there are upstream and downstream tests which are defined by the direction of electron flow. Figure 5(a) is the results of upstream EM test. In the upstream EM test, only Ta/TaN-3 diffusion barrier presents failure result. The failure mode of the upstream EM test on the structure with Ta/TaN-3 diffusion barrier is revealed by the XTEM image as shown in the inset of Figure 5(a). Obviously, the failure mode results from the upper Cu line opened by EM-induced void. The circle marks the initial location of void evolution. In this case, the EM-induced void is attributed to the weak interfacial adhesion between Cu line and Ta/TaN-3 diffusion barrier. Owing to TaN-3 and TaN-1 with the same N concentration, the crystalline behavior of Ta film deposited on TaN-3 is expected to form amorphous-like structure with the mixture of α- and β-phases. The interfacial bonding strength of Cu line and amorphous-like Ta film is relatively lower than that of Cu line and crystallized α-Ta film. During EM test, the interfacial bonding strength is highly required to resist electron-wind force [14–16]. Moreover, Ta/TaN-3 is thinner than Ta/TaN-1. For TaN/TaN-3 diffusion barrier with insufficient thickness and interfacial bonding strength,

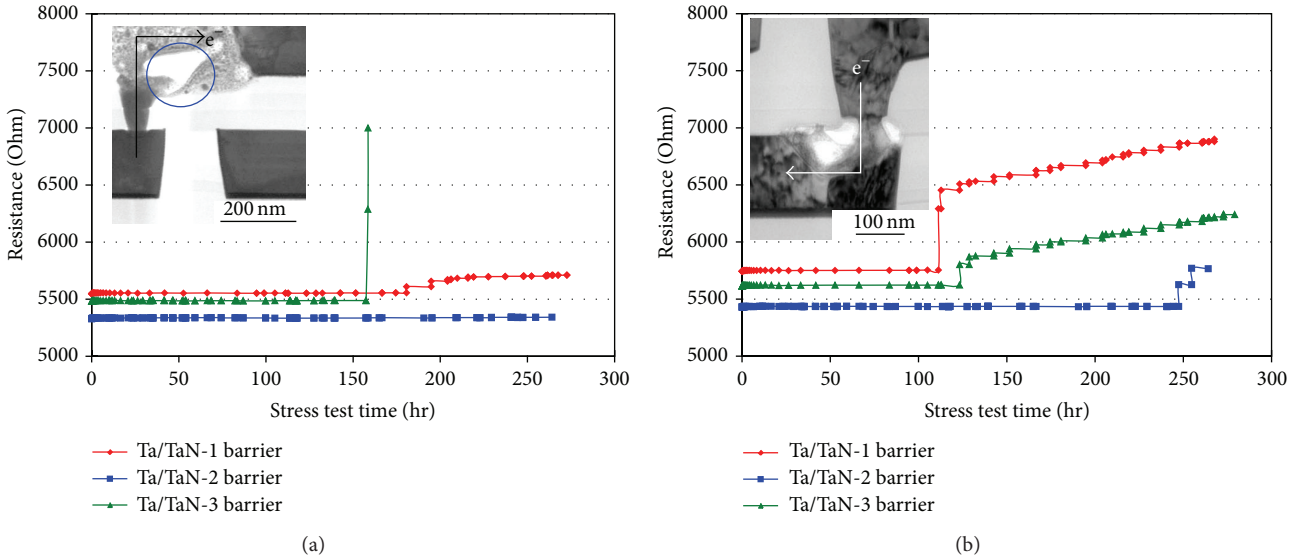

FIGURE 5: (a) Upstream and (b) downstream EM test results taken from the test Cu interconnection structures with Ta/TaN-1, Ta/TaN-2, and Ta/TaN-3 diffusion barriers. The insets of (a) and (b) are the XTEM images, showing the failure modes of the test Cu interconnection structures with Ta/TaN-3 and Ta/TaN-1 diffusion barriers, respectively.

the EM-induced void is eventually observed at the interface of Cu line and the diffusion barrier. Between Cu line and TaN/TaN-1 diffusion barrier, the interfacial bonding strength should be similar with the case of TaN/TaN-3 diffusion barrier. The resistance only gradually increases after the stress test time of 150 hours. However, the increment of resistance implies the appearance of EM-induced voids. In the test structure with TaN/TaN-1 diffusion barrier, the retardation of resistance increment and void evolution might be the contribution of the sufficient barrier thickness. For the structure with TaN/TaN-2 diffusion barrier, the elevation of resistance is barely observed after long stress test time. Undoubtedly, the strong interfacial bonding between Cu line and crystallized α-Ta successfully inhibits the appearance of EM-induced void. Figure 5(b) shows the results of downstream EM test. Remarkably, Ta/TaN-2 diffusion barrier gives the superior ability of EM resistance in Cu interconnection structure. The inset of Figure 5(b) is the representative XTEM image, showing the failure mode of the downstream test on the structure with Ta/TaN-1 diffusion barrier. The EM-induced voids are located around the corners of Cu via bottom and extend to the base of dielectric oxide layer. Usually, downstream EM test is stricter than upstream EM test. For downstream EM test, the EM resistance strongly depends on the resistance of diffusion barrier. Around the corners of Cu via bottom, the atomic flux divergence is much higher and easily reinforced by high resistance barrier. During downstream EM test, the interface of dielectric layer and Cu line firstly bears the brunt of electron-wind force. Since dielectric layer is totally amorphous, the interface of dielectric layer and Cu line is the weakest region in the overall Cu interconnection structure [16]. Suffering from high atomic flux divergence and naturally weak interface, the EM-induced voids finally deteriorate the interfaces of dielectric layers and Cu lines in the structures inserted with the high resistance barriers of Ta/TaN-1 and Ta/TaN-3. In Figure 5(b), the resistance increment of the structure with Ta/TaN-3 diffusion barrier is lower than that with Ta/TaN-1 diffusion barrier because Ta/TaN-3 diffusion barrier has lower resistance. With the possession of the lowest resistance, Ta/TaN-2 diffusion barrier significantly improves the EM resistance of Cu interconnection structure.

4. Conclusions

Ta/TaN bilayers deposited by SIP system have been systematically characterized by XRD and XTEM. The N concentration of amorphous TaN film shows remarkable influence on the crystalline feature of following Ta film. On TaN film with low N concentration, the overdeposited Ta film appears as an amorphous-like structure and comprises α- and β-phases. Increasing the N concentration of TaN underlayer successfully achieves pure crystallized α-phase in the subsequent Ta film. For the practical application, the utilization of α-Ta/TaN diffusion barrier efficiently reduces the KRc of Cu interconnection structure. The incorporation of α-Ta/TaN diffusion barrier significantly sustains Cu interconnection structure to resist the evolution of EM-induced voids in both up- and downstream tests. The electrical property and reliability of the overall Cu interconnection structure are certainly improved by the control of crystallized α-Ta/TaN diffusion barrier.

Conflict of Interests

The authors declare that there is no conflict of interests regarding the publication of this paper.

Acknowledgments

The authors would like to thank Instrument Technology Research Center for providing the assistance in material analyses. The material analyses were partially supported by National Science Council, Taiwan, under the Contract number NSC103-2622-E-492-010-CC3.

References

[1] M. Lane, R. H. Dauskardt, N. Krishna, and I. Hashim, "Adhesion and reliability of copper interconnects with Ta and TaN barrier layers," *Journal of Materials Research*, vol. 15, no. 1, pp. 203–211, 2000.

[2] R. Hubner, M. Hecker, N. Matterna et al., "Structure and thermal stability of graded Ta-TaN diffusion barriers between Cu and SiO_2," *Thin Solid Films*, vol. 437, no. 1-2, pp. 248–256, 2003.

[3] V. Sukharev, "Physically based simulation of electromigration-induced degradation mechanisms in dual-inlaid copper interconnects," *IEEE Transactions on Computer-Aided Design of Integrated Circuits and Systems*, vol. 24, no. 9, pp. 1326–1335, 2005.

[4] A. Roy and C. M. Tan, "Probing into the asymmetric nature of electromigration performance of submicron interconnect via structure," *Thin Solid Films*, vol. 515, no. 7-8, pp. 3867–3874, 2007.

[5] K.-H. Min, K.-C. Chun, and K.-B. Kim, "Comparative study of tantalum and tantalum nitrides (Ta_2N and TaN) as a diffusion barrier for Cu metallization," *Journal of Vacuum Science and Technology B: Microelectronics and Nanometer Structures*, vol. 14, no. 5, pp. 3263–3269, 1996.

[6] L. A. Clevenger, A. Mutscheller, J. M. E. Harper, C. Cabral Jr., and K. Barmak, "The relationship between deposition conditions, the beta to alpha phase transformation, and stress relaxation in tantalum thin films," *Journal of Applied Physics*, vol. 72, no. 10, pp. 4918–4924, 1992.

[7] S. L. Lee, M. Doxbeck, J. Mueller, M. Cipollo, and P. Cote, "Texture, structure and phase transformation in sputter beta tantalum coating," *Surface and Coatings Technology*, vol. 177-178, pp. 44–51, 2004.

[8] M. Stavrev, D. Fischer, C. Wenzel, K. Drescher, and N. Mattern, "Crystallographic and morphological characterization of reactively sputtered Ta, Ta–N and Ta–N–O thin films," *Thin Solid Films*, vol. 307, no. 1-2, pp. 79–88, 1997.

[9] J. H. Wang, L. J. Chen, Z. C. Lu, C. S. Hsiung, W. Y. Hsieh, and T. R. Yew, "Ta and Ta-N diffusion barriers sputtered with various N_2/Ar ratios for Cu metallization," *Journal of Vacuum Science and Technology B*, vol. 20, no. 4, pp. 1522–1526, 2002.

[10] Z. L. Yuan, D. H. Zhang, C. Y. Li, K. Prasad, and C. M. Tan, "Study of interactions between α-Ta films and SiO_2 under rapid thermal annealing," *Thin Solid Films*, vol. 462-463, pp. 279–283, 2004.

[11] Y.-S. Wang, C.-C. Hung, W.-H. Lee, S.-C. Chang, and Y.-L. Wang, "Under-layer behavior study of low resistance Ta/TaNx barrier film," *Thin Solid Films*, vol. 516, no. 16, pp. 5241–5243, 2008.

[12] J.-C. Tsao, C.-P. Liu, Y.-L. Wang, Y.-S. Wang, and K.-W. Chen, "Controlling Ta phase in Ta/TaN bilayer by surface pretreatment on TaN," *Journal of Physics and Chemistry of Solids*, vol. 69, no. 2-3, pp. 501–504, 2008.

[13] Z. H. Cao, K. Hu, and X. K. Meng, "Diffusion barrier properties of amorphous and nanocrystalline Ta films for Cu interconnects," *Journal of Applied Physics*, vol. 106, no. 11, Article ID 113513, 2009.

[14] P. Besser, A. Marathe, L. Zhao, M. Herrick, C. Capasso, and H. Kawasaki, "Optimizing the electromigration performance of copper interconnects," in *Proceedings of the IEEE International Electron Devices Meeting (IEDM '00)*, pp. 119–121, San Francisco, Calif, USA, December 2000.

[15] E. Zschech, M. A. Meyer, S. G. Mhaisalkar et al., "Effect of interface modification on EM-induced degradation mechanisms in copper interconnects," *Thin Solid Films*, vol. 504, no. 1-2, pp. 279–283, 2006.

[16] M. W. Lane, E. G. Liniger, and J. R. Lloyd, "Relationship between interfacial adhesion and electromigration in Cu metallization," *Journal of Applied Physics*, vol. 93, no. 3, pp. 1417–1421, 2003.